# Application of Pseudo Random Binary Sequences for Battery Impedance Estimation via Motor Drive Systems

28 May 2025

**Title:**

Application of Pseudo Random Binary
Sequences for Battery Impedance
Estimation via Motor Drive Systems

**Project:**

$4^{\text{th}}$ semester

**Project period:**

3 February to 28 May 2025

**Project group:**

MCE4-1027

**Study:**

Master of Science (MSc) in Engineering
(Energy Engineering with specialisation in
Mechatronic Control Engineering)

**Email:**

mbjerr20@student.aau.dk

**Supervisor:**

Erik Schaltz

**Number of pages:**

26 report

**Participants:**

Marcus Hoegh Bjerre

**Abstract:**

This project aims to investigate the use of
Pseudo Random Binary Sequence (PRBS)
signals for real time battery impedance es-
timation in systems where a battery powers
a motor drive. Traditional impedance meas-
urement methods like Electrochemical Im-
pedance Spectroscopy (EIS) are accurate
but impractical for online monitoring due
to their complexity and long measurement
times. PRBS excitation offers faster, more
implementation friendly alternative by en-
abling frequency domain analysis from time
domain signals. A PRBS signal is injec-
ted into the current reference of a Field
Oriented Control (FOC) structure driving
a Permanent Magnet Synchronous Machine
(PMSM). The resulting battery side current
and voltage are recorded and processed to
extract impedance using frequency domain
techniques. Simulations are performed on a
4-RC battery model with various PRBS con-
figurations to evaluate how bit length, clock
frequency and amplitude affect the quality
of the impedance estimation. Results show
that careful tuning of PRBS parameters is
essential to balance low frequency resolu-
tion, high frequency coverage and simula-
tion duration. While high bit lengths im-
prove diffusion region resolution, they sig-
nificantly increase test time. In contrast,
higher clock frequencies enhance high fre-
quency capture but reduce low frequency es-
timation and proposes design guidelines for
selecting PRBS parameters, laying ground-
work for future experimental validation.

# Resumé

På de seneste år har der været en stigende efterspørgsel på lithium-ion batterier inden for bilindustrien. Denne efterspørgsel er primært på baggrund af en stigende produktion af elektriske køretøjer. For enhver elektrisk bil findes der et system som måler og estimere vigtige batteri parametre og batteri tilstande, såsom ladetilstand og sundhedstilstand.

De konventionelle metoder til estimering af batteriets parameter er dog utilstrækkelige, når det kommer til nøjagtighed. Traditionel impedansspektroskopi (Electrochemical Impedance Spectroscopy, EIS) er derimod mere præcis, men ikke praktisk anvendelig til online måling. Pseudo Random Binary Sequence (PRBS) er blevet undersøgt af forskere som en mulig metode der er velegnet til online brug.

Dette projekts formål er derfor at undersøge hvordan PRBS kan designes og anvendes til impedans estimering i et motor drevet batteri system.

PRBS er en sekvens af genereret binære signaler, hvor signalets varighed kan bestemmes baseret på antallet af 'unit delay' blokke. Det spektrale indhold påvirkes delvist af antallet af 'unit delay', men også af signalets clock periode, hvilket er den tid der går, før signalet skifter værdi. Ved at justere på disse to parametre, er det derfor muligt at påvirke, hvilke frekvensområder af batteriets impedans der bliver undersøgt.

Der undersøges, hvordan et PRBS signal kan kombineres med motorens kontrol struktur for at excitere batteriet. PRBS signalet bliver implementeret i Field Oriented Control (FOC) som en forstyrrelse i $i_q$ strøm referencen. FOC kontrol strukturen styrer motoren, hvilket er en Permanent Magnet Synchronous Machine (PMSM). Motorens moment efterspørgsel bliver herefter brugt til at bestemme batteriets strøm.

En 4-RC batteri model bliver anvendt til at efterligne batteriets impedans dynamik. For at estimere parametrene i batteri modellen, analyseres impedansen målt fra et Electrochemical Impedance Spectroscopy (EIS) eksperiment. Værdierne kan bestemmes ud fra formen af halvcirkler i et Nyquist diagram. På baggrund af disse parameter opstilles der en teoretisk impedans. Denne teoretiske impedans model, bruges til at sammenligne med impedans data fra simulations resultater.

Adskillige PRBS konfigurationer bliver testet for at evaluere hvordan bit-længde, clock frekvens og amplituden af PRBS signal har effekt på kvaliteten af impedans estimering. Det viste sig, at større bit-længder positivt påvirkede det lav frekvente område af impedansen, men simulationstid og støj blev også større. En højere clock frekvens for PRBS signalet tilladte bedre impedans bestemmelse i de højfrekvente områder, men kom på bekostning af dårligere eller direkte ingen impedans bestemmelse i det lavfrekvente områder.

Design af PRBS afhænger derfor af hvilke frekvenser der er interesse for samt af systemets evne til at håndtere større datasæt, som kræver mere beregningsbyrde. Derudover bør det bemærkes, at eftersom der ikke er udført eksperimentelt arbejde kan adskillige faktorer som målestøj og korrekt skalering af PRBS signalets amplitude have en mere betydende effekt på den estimerede impedans kvalitet.

Fremtidigt arbejde bør fokusere på at implementere metoden i et fysisk setup, validere metoden og design valg af PRBS indstillinger.
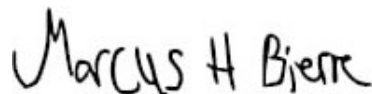
# Preface

This project is written by a $4^{\text{th}}$ semester master student, Marcus Hoegh Bjerre, studying Energy Engineering (Mechatronic Control Engineering) at Aalborg University. It is written in the period 3 February to 28 May 2025, under supervision of Erik Schaltz and with assistance from Farshid Naseri.

I would like to extend my thanks to Erik Schaltz and Farshid Naseri for all the help and advice given during the project period.

During the making of this project, the following programs have been used:

- Overleaf LaTeX— For text processing and layout of this report
- MathWorks MATLAB & Simulink — For calculations, simulations, calculations and data processing
- Draw.io — For diagrams and illustrations

_____

Marcus Hoegh Bjerre

Aalborg University, 28 May 2025

# Nomenclature

## Symbols

| Symbol | Definition | Unit |
|:---:|:---:|:---:|
| $C$ | Capacitance | F |
| $f_c$ | PRBS clock frequency | Hz |
| $f_{max}$ | Maximum PRBS frequency | Hz |
| $f_{min}$ | Minimum PRBS frequency | Hz |
| $I(t)$ | Current (time domain) | A |
| $n$ | Bit length | − |
| $N$ | PRBS sequence length | − |
| $N_{cycles}$ | Number of PRBS cycles | − |
| $R$ | Resistance | Ω |
| $T_c$ | Clock period | s |
| $T_{PRBS}$ | PRBS duration of 1 period | s |
| $T_{total}$ | Total PRBS duration | s |
| $V(t)$ | Voltage (time domain) | A |
| $Z(j\omega)$ | Impedance in frequency domain | Ω |
| $\omega$ | Angular frequency | rad/s |

# Abbreviations

| Abbreviation | Definition |
| --- | --- |
| BMS | Battery Management System |
| ECM | Equivalent Circuit Model |
| EIS | Electrochemical Impedance Spectroscopy |
| EV | Electric Vehicle |
| FFT | Fast Fourier Transform |
| FOC | Field Oriented Control |
| PLL | Phase Locked Loop |
| PMSM | Permanent Magnet Synchronous Machine |
| PRBS | Pseudo Random Binary Sequence |
| SEI | Solid Electrolyte Interphase |
| SoC | State of Charge |
| SoH | State of Health |
| SVM | Space Vector Modulation |
| XQR | Exclusive OR logic gate |

# Contents

# Introduction 1

In recent years, there has been a growing demand for lithium-ion (Li-ion) batteries in the automotive industry as a means of energy storage for propulsion. In 2022 alone, the demand reached 550 GWh, representing a 65% increase from the previous year. This growth is primarily driven by the rising production of electric vehicles (EVs) [1]. Li-ion batteries have become the preferred energy storage technology in EVs due to their high energy density, relatively low self-discharge, and favorable performance characteristics [2]. To ensure safe and reliable operation, these batteries are typically equipped with a battery management system (BMS) that monitors key parameters such as voltage, temperature and current.

Predicting the life expectancy and degradation behavior of Li-ion batteries remains a significant challenge. This is primarily due to the complexity of the ageing mechanisms, which is influenced by multiple factors such as temperature, current load, and charge/discharge cycles. Since the battery pack is often the most expensive component of an EV, it also directly impacts key performance metrics like power output and driving range. It is therefore crucial to ensure that its usage is optimized throughout its lifecycle. To achieve this, precise monitoring and accurate estimation of battery states are essential in order to avoid premature degradation and maximize performance and longevity.

Conventional BMS approaches use measurements of battery voltage, current and temperature to infer battery states, such as State of Charge (SoC) and State of Health (SoH) [3]. Achieving high accuracy with these methods is challenging since the parameters measured relate to SoC and SoH in non-linear ways [3]. Traditional impedance spectroscopy methods are more accurate but require expensive equipment, lengthy frequency sweeps and are bulky, limiting their application in EVs.

Recent studies in Pseudo Random Binary Sequence (PRBS) impedance spectroscopy has shown that PRBS method can bring the benefits of Electrochemical Impedance Spectroscopy (EIS) into real time vehicle monitoring [3]. This method is attractive due to their low measurement time and relatively good accuracy compared to alternatives [3], and the fact that it does not require any dedicated and costly hardware.

This report aims to develop and evaluate a method for online battery impedance estimation using PRBS signals. A particular focus will be placed on analyzing how the settings of the PRBS signal affect the quality of the extracted impedance. Based on these findings, the project will provide guidelines for choosing PRBS settings that achieve accurate results and a high signal-to-noise ratio. The ultimate goal is to offer a real time impedance estimation method suitable for electrical vehicles, potentially improving battery state estimation without the drawbacks of traditional approaches.

# Problem Statement 2

Battery state estimation is a key function of the BMS, where accurate monitoring helps ensure safe operation, performance, and longevity. The battery's impedance provides valuable insight into internal electrochemical processes, including degradation mechanisms.

Impedance data can be used to extract important information such as SoH and remaining useful life. These indicators are crucial for predicting ageing and determining whether a battery pack can continue operating effectively. Since EIS is unsuitable for online use, PRBS signals have been explored as a practical alternative for estimating impedance during regular operation.

This project aims to address the following question:

*How should PRBS signals be designed and configured to enable accurate battery impedance estimation in a motor driven system?*

## Objectives

To answer the problem statement, the following research goals are set:

- Analyse how different PRBS configurations (bit length, clock frequency, amplitude) affect the frequency content and impedance estimation quality
- Investigate how PRBS signals can be injected into the motor control structure
- Simulate the battery response under PRBS injected motor drive conditions using a PMSM model
- Propose a set of practical guidelines for selecting PRBS parameters for impedance estimation

# Battery Impedance Introduction <span style="font-size:3em">3</span>

Impedance describes how an electrical circuit resists the flow of alternating current (AC), expanding the concept of resistance to account for frequency-dependent effects. Unlike electrical resistance, impedance varies with frequency and includes both resistive and reactive components. This frequency dependence allows for a more detailed understanding of dynamic behaviour, particularly when analysed in the frequency domain.

This chapter introduces the concept of Electrochemical Impedance Spectroscopy (EIS) and how it can be used to characterise battery behaviour. Furthermore, it outlines how a battery model can be constructed to replicate an impedance plot, enabling accurate simulation of battery dynamics.

## 3.1   Electrochemical Impedance Spectroscopy

Electrochemical Impedance Spectroscopy (EIS) is a technique used to extract frequency-domain information from an electrochemical system by measuring its impedance. The method involves perturbing the system in steady state with a small sinusoidal excitation, either in the form of an AC voltage or current, across a range of frequencies. The system's response occurs at the same frequency but is typically phase shifted [4]. For example, an AC current excitation may be represented as:

$$I(t) = I \sin{(\omega t)} \tag{3.1}$$

and the resulting voltage response as:

$$V(t) = V \cos{(\omega t + \phi)} \tag{3.2}$$

The measured voltage and current over the frequency range are used to compute the impedance:

$$Z(j\omega) = \frac{V(j\omega)}{I(j\omega)} \tag{3.3}$$

These signals are then transformed into the frequency domain, typically using a Fast Fourier Transform (FFT), yielding both the magnitude and phase of the impedance. This frequency domain data is commonly represented by Bode or Nyquist plots, which reveal key characteristics of the system's dynamic behaviour.

In case of batteries, such plots can be used to interpret electrochemical processes at different frequency ranges. Figure 3.1 shows a Nyquist plot based on the impedance data from a 3.2 V 10 Ah lithium iron phosphate $LiFePO_4$ battery cell from A&S Power. The data illustrates the impedance behaviour at 90% state of charge (SoC) across four different temperatures.
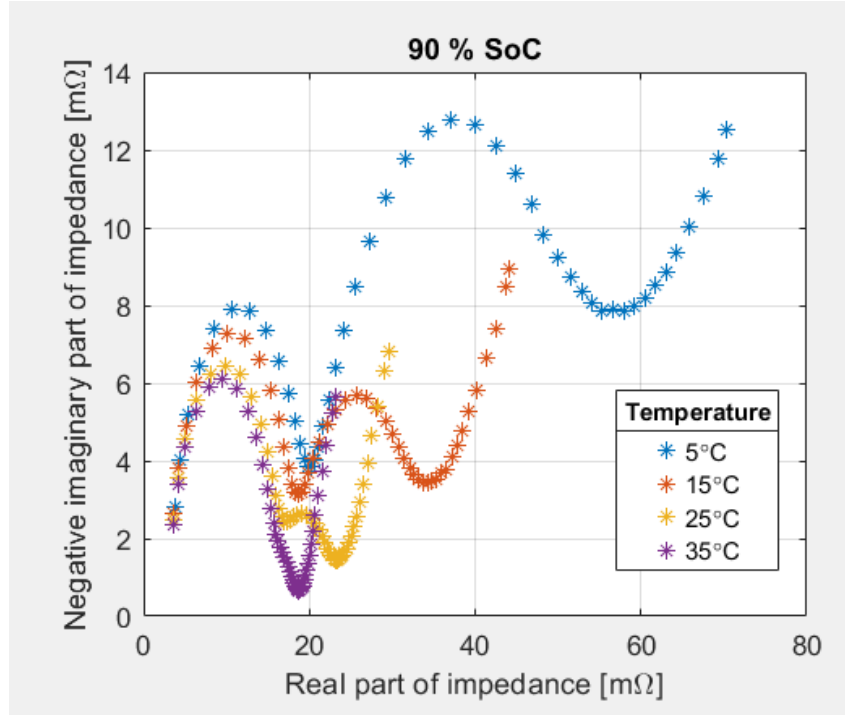
**Figure 3.1.** Nyquist plot of LiFePO$_4$ cell at 90% SoC for varying temperatures.

As seen in the figure, temperature has a significant influence on the impedance spectrum. At higher temperatures, the semi circle associated with the charge transfer resistance becomes less pronounced and overall impedance tends to decrease. This is due to the increased ionic mobility and accelerated electrochemical reactions within the cell. In contrast, lower temperatures slow these processes, increasing both resistance and diffusion related effects.

In addition to temperature, other factors such as SoC, SoH, and ageing also affect the impedance characteristics. These factors should be considered when evaluating impedance data, particularly when comparing results across different battery conditions.

Different electrical components have different impedance values attributed to them. A table can be seen below listing some of the more common electrical components with their impedance. To understand why impedance takes different shapes in the Nyquist plot, it is useful to recall that different electrical components contribute characteristic impedance responses. Table 3.1 summarises the idealised impedance expressions of common elements found in equivalent battery models.

**Table 3.1.** Impedance of common electrical components.

| Component | Impedance |
|:---:|:---:|
| Resistor | $Z_R = R$ |
| Inductor | $Z_L = j\omega L$ |
| Capacitor | $Z_C = 1/j\omega C$ |
| Warburg Element | $Z_W = W/j\omega^{0.5}$ |

From this, it can be observed that resistors are frequency independent and contribute only to the real part of the impedance. Capacitors and Warburg elements, on the other hand, exhibit frequency dependant behaviour and contribute negatively to the imaginary part. Inductors contribute positively to the imaginary part.

To relate these components to physical battery behaviour, it can be insightful to overlay a Nyquist plot with a battery model, as demonstrated in [5], shown in Figure 3.2. This representation helps clarify which physical process dominate in different frequency regions.
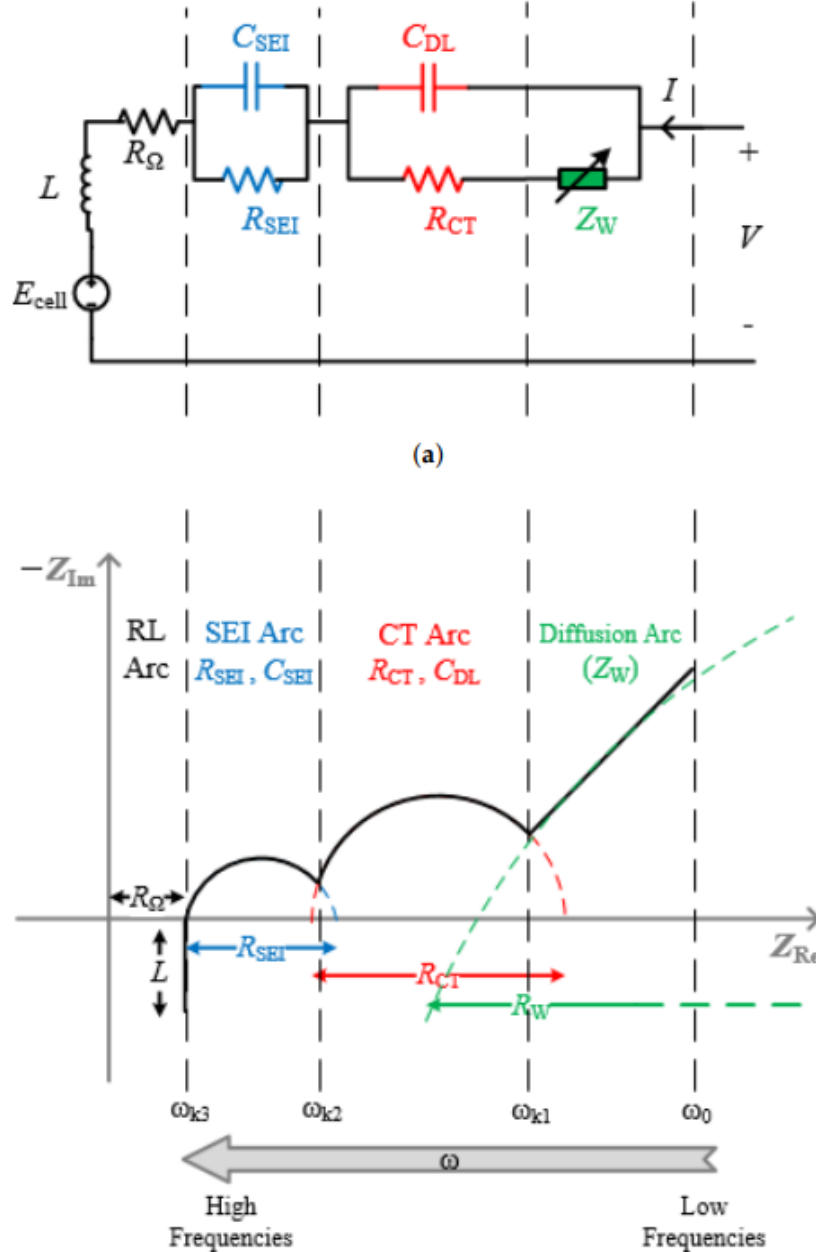


**Figure 3.2.** Nyquist plot and equivalent circuit model [5].

Each process in the battery occurs simultaneously but operates on a different time scale, and therefore becomes visible at a different frequency range in the impedance spectrum:

- **High frequency** ($\omega_{k3}$, kHz)
  This region reflects the ohmic resistance of the battery and any inductive effects. The ohmic resistance appears as a purely real component, while inductive effects appear as a positive imaginary component at very high frequencies.
- **Mid frequency** ($\omega_{k2}$ **to** $\omega_{k1}$, Hz)
  The first semi circle is typically associated with the solid electrolyte interphase (SEI) layer, represented by a parallel combination of $R_{SEI}$ and $C_{SEI}$. The second semi circle corresponds to the charge transfer resistance and double layer capacitance at the electrode/electrolyte interface, modelled by $R_{CT}$ and $C_{DL}$.
- **Low frequency** ($\omega_{k1}$ **to** $\omega_0$, mHz)
  Low frequency represents diffusion related impedance. The Warburg element $Z_W$ captures the gradual movement of lithium ions through the electrode material. This appears as a diagonal line with a slope near 45°.

To simulate the impedance of a battery over a wide frequency range, it is necessary to develop a model that accurately reproduces the behaviour observed in each of these regions. This is typically done using equivalent circuit models (ECMs), which are introduced in the following section.

## 3.2   Equivalent Circuit Models

Equivalent Circuit Models (ECMs) are widely used to represent the dynamic behaviour of batteries and simulate their impedance response, as demonstrated in the previous section. The accuracy of the simulated impedance depends strongly on the complexity of the model. More advanced models typically yield higher accuracy by capturing additional electrochemical phenomena, though this comes at the cost of increased parametrisation and computational load.

A typical battery model can be constructed using an ohmic resistance in series with one or more RC pairs, each representing a process with a distinct time constant. A generalised model with $n$ RC pairs is shown in Figure 3.3.
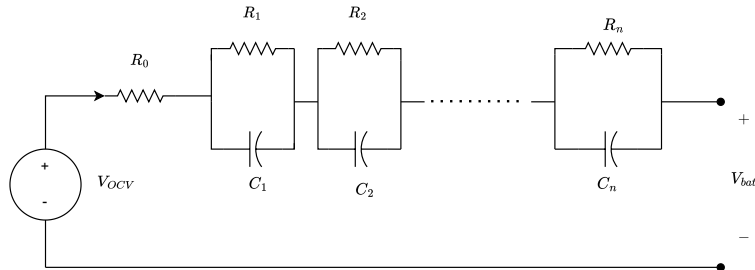


***Figure 3.3.*** Generalised battery model with multiple RC pairs.

As mentioned in Section 3.1, different electrical components possesses different impedance characteristics. The Warburg element, is more difficult to represent in a time domain simulation, as there is no simple element to model it. Instead, a series of RC pairs that span multiple time constants can be used to approximate the impedance in the low frequency area.

Parameter estimation from EIS data involves interpreting specific features of the Nyquist plot to extract resistance and capacitance values for each RC pair in the equivalent circuit. A common approach is to identify the high frequency intercept of the real axis, which corresponds to the ohmic resistance $R_0$ [5]:

$$R_0 = \min(Re(Z)) \tag{3.4}$$

For the mid frequency arcs appear as semi circles on the Nyquist plot. Their diameters corresponds to resistances $R_{CT}$ and $R_{SEI}$, and their peak frequencies can be used to estimate associated capacitances. At the peak of each arc, the following relationships hold [5]:

$$R = 2|Im(Z)|, \qquad f_{peak} = \frac{1}{2\pi RC} \tag{3.5}$$

Hence, at the peak of the CT arc, the charge transfer resistance $R_{CT}$ and double layer capacitance $C_{DL}$ can be estimated as:

$$R_{CT} = 2|Im(Z_{CT})|, \qquad C_{DL} = \frac{1}{2\pi f_{CT,peak} R_{CT}} \tag{3.6}$$

Similarly, the SEI resistance and capacitance can be estimated using:

$$R_{SEI} = 2|Im(Z_{SEI})|, \qquad C_{SEI} = \frac{1}{2\pi f_{SEI,peak} R_{SEI}} \tag{3.7}$$

This method ignores the effect of the Warburg impedance and assumes each arc can be approximated by a simple RC pair. This method can become unreliable if the arcs are not clearly separated, which happens at higher temperatures. Furthermore since it ignores the Warburg element, the overlap from the diffusion will have an effect on the semi circle approximation. Therefore a second approach was used to refine the parameters.

The refined parameters values were obtained by fitting a n-RC equivalent circuit model to complex impedance data using Matlab 'lsqnonlin' function [5]. This model has the form:

$$Z(j\omega) = R_0 + \frac{R_1}{1 + j\omega R_1 C_1} + \frac{R_2}{1 + j\omega R_2 C_2} + ... + \frac{R_n}{1 + j\omega R_n C_n} \tag{3.8}$$

A cost function is then implemented to minimise the sum of squared differences between the measured and modelled impedances over all frequency points.

$$\hat{\theta} = \arg\min_{\theta} \sum_{k=1}^{N} |Z_{\text{measured}}(\omega_k) - Z_{\text{model}}(\omega_k, \theta)|^2 \tag{3.9}$$

where $\theta = [R_0, R_1, C_1, R_2, C_2]$.

# Design of PRBS Signals for Impedance Estimation $4$

In order to estimate battery impedance during operation, a excitation signal is required. Pseudo Random Binary Sequence (PRBS) is one excitation method, that can be tailored to excite specific frequency ranges.

This chapter introduces the concept of PRBS, explains how it is generated, explores its frequency characteristics and mentions key design considerations for its application in battery system identification.

## 4.1   Introduction to PRBS

A Pseudo Random Binary Sequence (PRBS) is a binary signal, switching between unipolar values 0 and 1 or modified to bipolar values $\pm 1$. It is commonly used as a form of system identification by exciting dynamic systems, due to its similarity to white noise over a limited frequency range. By adjusting the PRBS parameters (such as bit length and clock frequency), the excitation can be shaped to match a system under test. When applied to a system, PRBS enables frequency analysis by allowing extraction of the system's frequency response within the excited bandwidth.

## 4.2   PRBS Generator Structure

The 'pseudo-random' part of the name refers to how the sequence is generated, as the sequence is not completely random, but is deterministic and repeatable. Typically, this sequence is generated using a circuit called a linear feedback shift register, which can be built using a series of unit delays and XOR logic gates. An example of a 9-bit PRBS generator is shown in Figure 4.1.
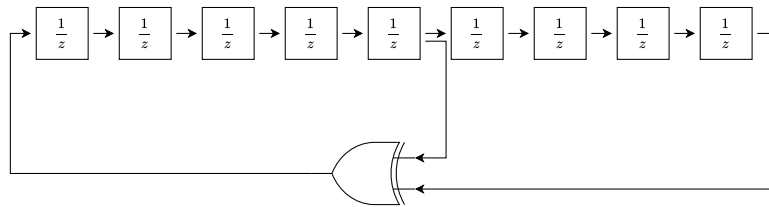


*Figure 4.1.* 9-bit PRBS generator.

The number of delays, often referred to as the bit length $n$, determines the length of the generated sequence and will repeat after $N$ states [6].

$$N = 2^n - 1 \tag{4.1}$$

A 9-bit PRBS generator will therefore produce a sequence of 511 bits before repeating.

The PRBS signal updates at a fixed interval determined by the time delay $T_c$, which sets the clock frequency $f_c$ of the signal:

$$T_c = \frac{1}{f_c} \tag{4.2}$$

For example, setting $T_c = 0.1s$ results in a PRBS signal with a clock frequency of $f_c = 10Hz$, as illustrated below:



*(a)* Full period of a 9-bit 10 Hz signal.        *(b)* First 5 seconds of the signal.
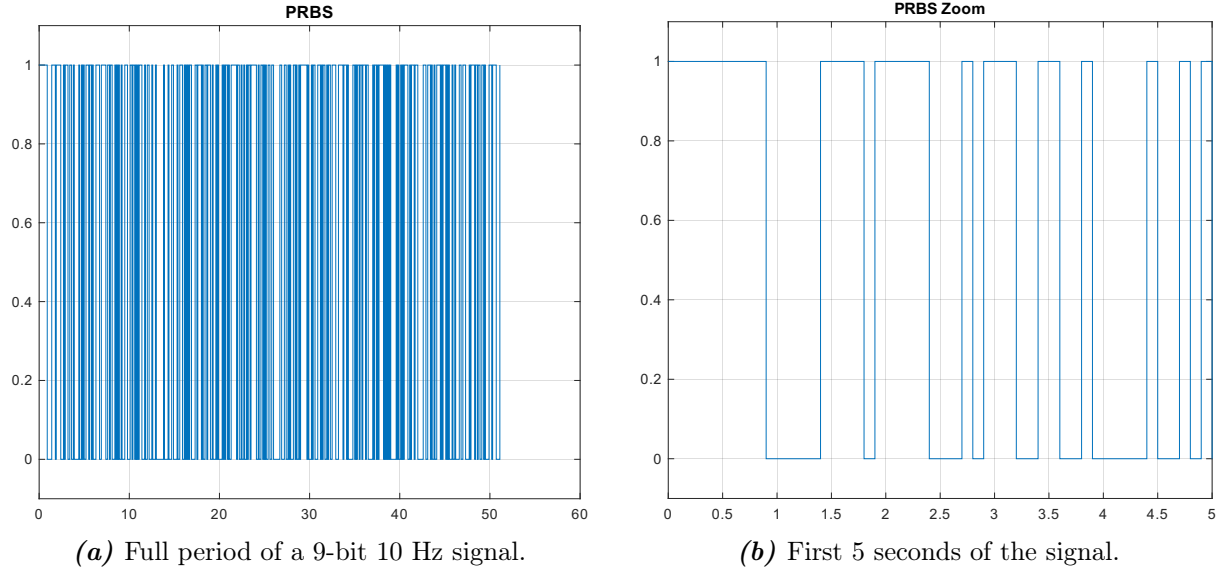
*Figure 4.2.* Overview of PRBS in time and frequency domain

The time for the sequence is a product of the sequence length and $T_c$, which in this example becomes 51.1 s. This sequence can be repeated multiple times to obtain several complete cycles. The total time to complete all cycles $T_{total}$ depends on the length of one PRBS cycle and the number of repetitions. A single PRBS period has a duration given by:

$$T_{PRBS} = NT_c, \qquad T_{total} = T_{PRBS}N_{cycles} \tag{4.3}$$

here $N_{cycles}$ are the number of repeated sequences. As seen from Equation (4.1), increasing the bit length $n$ increased $N$ exponentially, which can quickly lead to longer PRBS sequences and increased simulation time.

## 4.3   Bandwidth of PRBS

The clock frequency of a PRBS determines the rate at which the signal changes, and it also directly affects the frequency content. The usable frequency range of a PRBS lies between a minimum frequency $f_{min}$ and a maximum frequency $f_{max}$. The minimum frequency corresponds to the fundamental frequency of the periodic sequence and is given by [6]:

$$f_{min} = \frac{f_c}{N} \tag{4.4}$$

The maximum frequency is typically defined as the point where the power spectrum of the PRBS drops by 3 dB from its flat region. For a PRBS signal, this can be approximated as [6]:

$$f_{max} \approx \frac{f_c}{3} \tag{4.5}$$
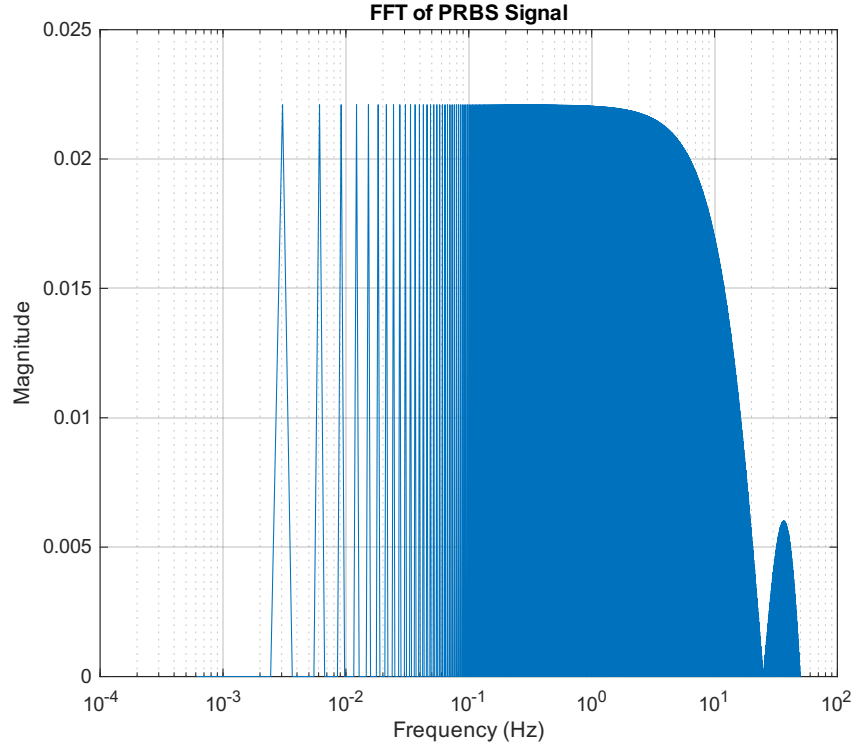


*Figure 4.3.* Power spectrum of a PRBS.

A higher clock frequency will increase both the minimum frequency and maximum frequency to target higher overall frequencies. Since only the clock frequency has an effect on $f_{max}$, a clock frequency can be found that targets a desired max frequency can be found and afterwards try and decrease the minimum frequency by choosing a higher bit length. The table below shows a range of clock frequencies and the corresponding maximum frequency.

*Table 4.1.* Minimum and maximum frequencies for various bit lengths and clock frequencies.

| Bit Length (n) | $f_{\min}$ [Hz] at $T_c$=0.1 | $f_{\min}$ [Hz] at $T_c$=0.05 | $f_{\min}$ [Hz] at $T_c$=0.01 | $f_{\min}$ [Hz] at $T_c$=0.005 | $f_{\min}$ [Hz] at $T_c$=0.001 |
|---|---|---|---|---|---|
| 4 | 0.6667 | 1.3333 | 6.6667 | 13.3333 | 66.6667 |
| 5 | 0.3226 | 0.6452 | 3.2258 | 6.4516 | 32.2581 |
| 6 | 0.1587 | 0.3175 | 1.5873 | 3.1746 | 15.8730 |
| 7 | 0.0787 | 0.1575 | 0.7874 | 1.5748 | 7.8740 |
| 8 | 0.0392 | 0.0784 | 0.3922 | 0.7843 | 3.9216 |
| 9 | 0.0196 | 0.0391 | 0.1957 | 0.3914 | 1.9569 |
| 10 | 0.0098 | 0.0195 | 0.0978 | 0.1955 | 0.9775 |
| $f_{max}$ [Hz] | 3.33 | 6.67 | 33.33 | 66.67 | 333.33 |

## 4.4    Design Considerations

When designing a PRBS signal for battery impedance estimation, several key parameters must be considered. These parameters determine the frequency content, duration, and amplitude of the excitation signal, and they involve trade-offs that affect the accuracy and resolution of the impedance measurement.

The most important design parameters include:

- Bit length ($n$)
  Increasing the bit length helps increase lower frequency resolution, as it results in a lower $f_{min}$. A tradeof is that increasing the bit length will also increase the sequence length and increase simulation time and increase the noise.
- Clock Frequency ($f_c$)
  The clock frequency affects both $f_{min}$ and $f_{max}$. Increasing $f_c$, raises both $f_{min}$ and $f_{max}$, pushing the spectrum towards higher frequencies, while also shortening the simulation time. To capture the high frequency ohmic region, a high $f_c$ would be needed. Opposite of that to capture the low frequency diffusion region, a low $f_c$ is needed.
- Amplitude Scaling
  The amplitude of the PRBS signal is trade off between the impedance estimation quality and safety of the battery. Higher amplitude perturbation improves the signal quality, but may introduce more non-linear effects. As such the amplitude is a balancing act to keep a high signal quality while avoiding disturbing the systems stability.
- Number of PRBS Periods
  Multiple PRBS periods helps reduce noise via averaging, but comes at the cost of a longer test time. Repeating the PRBS excitation multiple times and averaging improves quality of the impedance spectrum but also results in longer simulation time.

# Methodology 5

## 5.1 Battery Model Setup

The battery impedance model used throughout this project is based on a 4-RC equivalent circuit model, as shown in Figure 5.1. This model consists of an ohmic resistance $R_0$ in series with four parallel RC branches, each representing a dynamic process within the battery across different time constants. This approach allows the model to capture high frequency behaviour as well as low frequency diffusion effects.
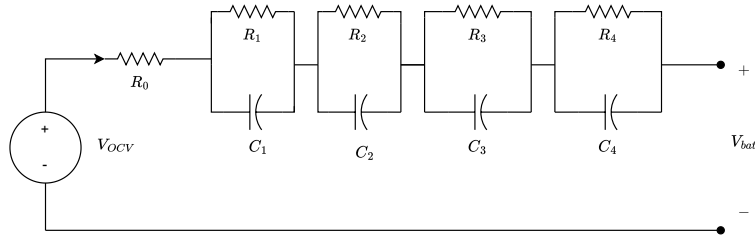
***Figure 5.1.*** 4-RC battery model used to represent impedance across a wide frequency range.

While a simpler 2-RC model was initially considered, it did not adequately capture the low frequency diffusion tail observed in Nyquist plots. Therefore, the 4-RC model was selected and used exclusively in all simulations and impedance estimations presented in this report.

To validate the model structure, an ideal impedance was calculated based on the estimated 4RC parameters using the parameter estimation methods described in Section 3.2. This theoretical impedance was implemented using a transfer function based approach in MATLAB. The result is used as a reference to assess the accuracy of simulated impedance responses.

Figure 5.2 compares the impedance measured from an EIS test with the theoretical impedance from the 4-RC model.
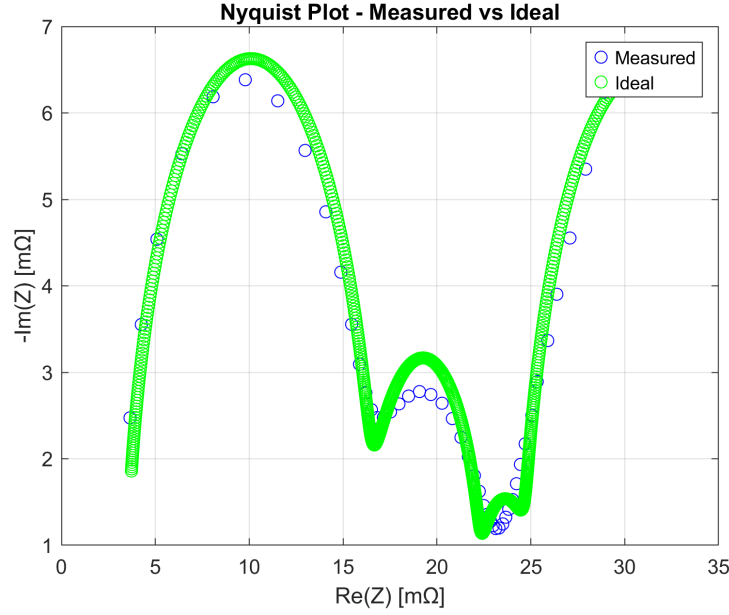
***Figure 5.2.*** Comparison between measured EIS data and ideal impedance based on estimated 4RC parameters.

Simulations will be compared against the ideal impedance. Meanwhile, experimental impedance data can be compared with the EIS impedance.

The battery model was implemented in Simulink and designed to be both temperature and SoC dependent, using lookup tables. Breakpoints were defined at the following values:

- **Temperature**: 5°C, 15°C, 25°C and 35°C
- **State of Charge**: 90%, 70%, 50%, 30% and 10%

However, to simplify simulations and maintain focus on the PRBS injection strategy, the temperature was fixed at 25°C and the input SoC was set at 50% throughout all the simulation scenarios.

The primary objective of this modelling approach is to estimate battery impedance under dynamic load conditions that mimic real world operation. Although impedance data can be further utilised for estimating battery SoH, aging analysis and diagnostics, such applications are beyond the scope of this project.

## 5.2   Motor Drive Implementation

The motor drive system is based on Field Oriented Control (FOC) structure applied to a Permanent Magnet Synchronous Machine (PMSM). The control scheme consists of an outer speed control loop and an inner current control loop, enabling independent control of torque and magnetic flux through $i_d$ and $i_q$ current components.

This model builds upon previous work from an earlier project [7], which developed and validated the PMSM model and its FOC implementation. Therefore, detailed derivation and controller tuning are not repeated here. Instead, this section focuses on how PRBS excitation is injected into the motor controller loop to perturb the battery current and enable impedance estimation.
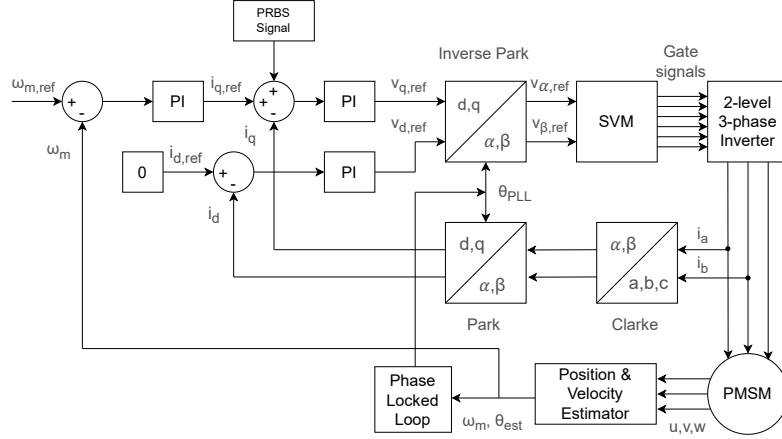


**Figure 5.3.** Field-Oriented Control structure of the PMSM with PRBS injection into $i_{q,\text{ref}}$.

As shown in Figure 5.3, the PRBS signal is injected as a disturbance onto $i_{q,ref}$ signal. Since $i_q$ is directly responsible for torque production, this causes small fluctuations in the motor torque, which in turn modulate the mechanical load and the power drawn from the battery. This mechanism enables the PRBS excitation to propagate through the system and affect the battery side current, which is necessary for impedance identification.

The PRBS signal is generated separately and scaled using a tunable gain block to ensure a suitable amplitude. The amplitude is chosen to be high enough to yield a good signal to noise ratio in the battery current, while still keeping the system within a linear operating range to avoid instability or nonlinear distortions.

The battery current is derived from the motor's power demand, assuming an ideal three-phase inverter. The calculated mechanical power is divided by the battery voltage, which is provided by the battery model in simulation. This approach allows the PRBS induced dynamics to pass through the full electromechanical chain and affect the battery side current in a realistic manner.

## 5.3 Post Processing

The battery voltage and current are measured at the DC side of the system and logged during simulation. This data is exported to MATLAB using `To Workspace` blocks for post processing. the objective is to extract the battery impedance by transforming the measured time domain signals into the frequency domain and computing their ratio.

Before transforming the signal to the frequency domain, a window function is applied to the signals. When applying Fast Fourier Transform (FFT), it can introduce spectral leakage. Spectral leakage results in unwanted frequency components in the spectrum. To avoid this, a

window is applied to smooth out the edges of a subset of the data inside the window.  Therefore the Hann function is applied to reduce spectral leakage before performing FFT.

In order to transform the time domain data into the frequency domain, FFT is applied to the time domain signals.  The FFT output includes both positive and negative frequencies.

A one-sided FFT is then computed to obtain the magnitude and phase of the voltage and current spectra.  Since the FFT output includes both positive and negative frequencies, only the positive half is retained, as the negative spectrum is symmetric and does not add new information.

Impedance is then calculated in the frequency domain using complex ratio between voltage and current, as defined by:

$$Z(j\omega) = \frac{V(j\omega)}{I(j\omega)} \tag{5.1}$$

This calculated impedance is plotted using both Bode and Nyquist plots for analysis.  These plots are used to compare the simulated impedance with the ideal theoretical impedance derived from the 4RC model, as well as the experimental EIS reference data when available.

# Results 6

This chapter presents the simulation results from injecting PRBS signals into the motor-driven battery system. A baseline simulation configuration is established to evaluate the effect of individual PRBS parameters. The performance of each configuration is assessed in terms of the frequency content of the input signal and the accuracy of the extracted impedance spectrum.

The baseline setup uses:

- A 9-bit PRBS generator
- A $f_c$ of 100 Hz ($T_c = 0.01$ s)
- Five full PRBS periods
- Amplitude scaling of 1.2

This setup is used to establish a consistent foundation for evaluating different PRBS configurations. The following figure shows the Nyquist plot and FFT for the baseline setup.
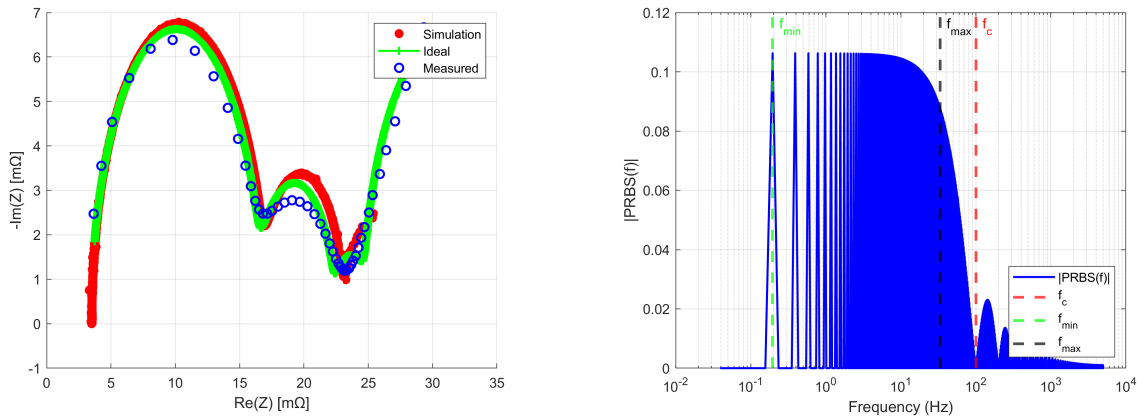


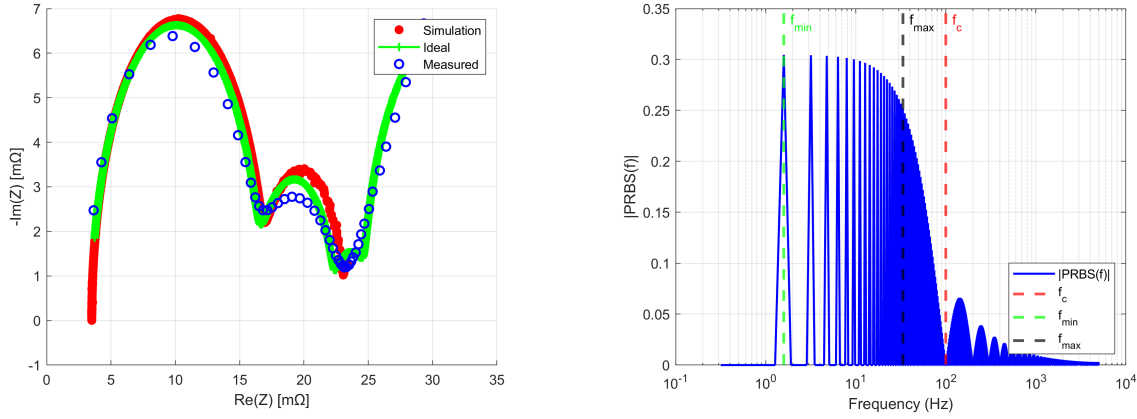*Figure 6.1.* Nyquist and FFT plot of the 9-bit generator.

From the figure it can be seen that the baseline configuration captures both semi circles of the Nyquist plot, and begins to enter the diffusion region.

This configuration serves as a reference to isolate the influence of how changes in individual PRBS parameter affect the quality of the impedance estimation. The subsequent simulations vary one parameter at a time, such as PRBS bit length, clock frequency or amplitude while keeping all other parameters constant.

## 6.1   Effect of Bit Length

To study the effect of bit length $n$, simulations were run using a 6-bit, 9-bit and 12-bit PRBS generators, all at a fixed clock period $T_c = 0.01$ s. The objective is to observe how changes in $n$ impact the minimum frequency and thereby the resolution in the low frequency diffusion region of the Nyquist plot.
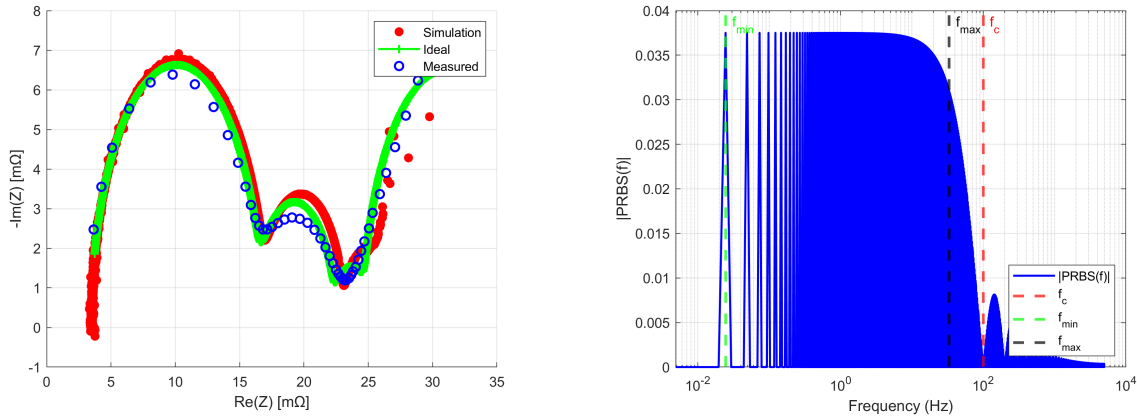
**6-bit PRBS**



***Figure 6.2.*** Nyquist and FFT plot of the 6-bit generator.

As shown in Figure 6.2, the 6-bit PRBS captures the two semi circles of the impedance spectrum but fails to resolve the low frequency diffusion tail. The FFT confirms the lack of low frequency content below 1.5 Hz.

**12-bit PRBS**



***Figure 6.3.*** Nyquist and FFT plot of the 12-bit generator.

The 12-bit configuration achieves $f_{min} \approx 0.024$ Hz, significantly improving resolution in the diffusion region. However, this comes at a cost of longer sequence duration (205 s), which increases simulation time and introduces higher noise, particularly in the high frequency region.

*Table 6.1.* PRBS duration and minimum frequency for different bit lengths at a fixed clock period of $T_c = 0.01$ s.

| Bit Length $n$ | PRBS Duration (s) | $f_{min}$ (Hz) | $f_{max}$ (Hz) |
|:---:|:---:|:---:|:---:|
| 6 | 3.15 | 1.59 | 33.33 |
| 9 | 25.55 | 0.196 | 33.33 |
| 12 | 204.75 | 0.0244 | 33.33 |

## 6.2 Effect of Clock Frequency

To isolate the effect of clock frequency, the PRBS bit length is fixed at 9. The baseline simulation uses a clock period of $T_c = 0.01$ s, which corresponds to a clock frequency of 100 Hz. Since this baseline case has already been presented, it is omitted here.

Instead, this section focuses on comparing two alternative clock settings: $T_c = 0.1$ s and $T_c = 0.001$ s. These configurations allow us to evaluate how shifting the clock frequency affects the bandwidth and the impedance quality, particularly in the ohmic and diffusion regions.

$T_c = 0.1s$ **- low clock frequency**
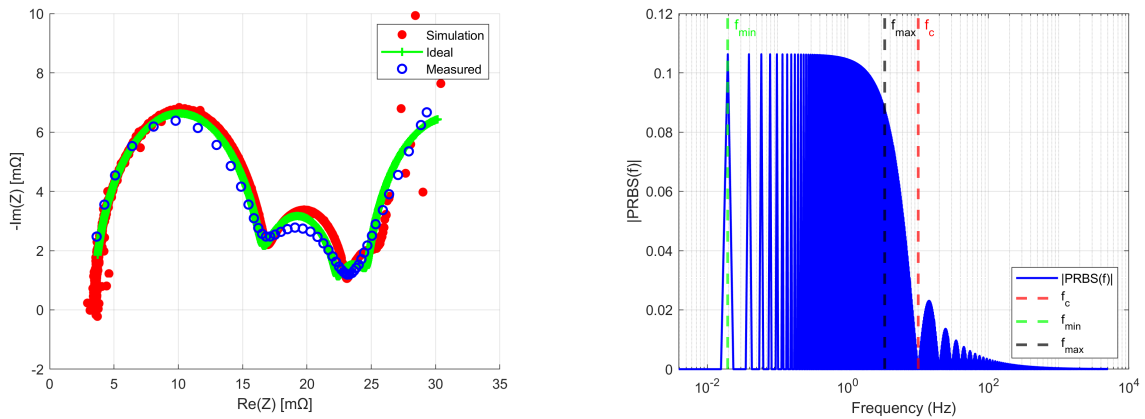


*Figure 6.4.* Nyquist and FFT plot of the 9-bit generator with $T_c = 0.1$ s.

As seen in Figure 6.4, the low clock frequency results in a narrower frequency band with a maximum frequency of approximately 3.33 Hz. This leads to a strong emphasis on the low frequency region of the Nyquist plot, where the Warburg diffusion line becomes more apparent.

$T_c = 0.001$ s - High clock frequency
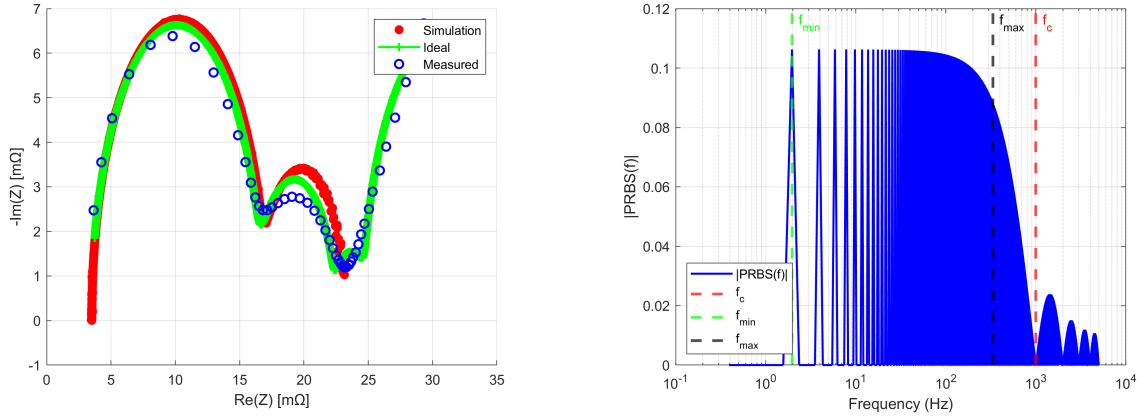


***Figure 6.5.*** Nyquist and FFT plot of the 9-bit generator with $T_c = 0.001$ s.

In constrast, the configuration with $T_c = 0.001$ s produces a wideband PRBS signal reaching up to 333 Hz. This allows the Nyquist plot to capture the high frequency ohmic region more accuratly. However, the lower frequency content is sacrificed, as $f_{min}$ increases to 1.96 Hz. This limits the ability to resolve the diffusion tail, making the low frequency estimation poor.

***Table 6.2.*** PRBS duration and frequency bounds for different clock periods $t_c$ at a fixed bit length of $n = 9$.

| Clock Period $T_c$ (s) | PRBS Duration (s) | $f_{\mathbf{min}}$ (Hz) | $f_{\mathbf{max}}$ (Hz) |
|:---:|:---:|:---:|:---:|
| 0.1 | 51.1 | 0.0196 | 3.33 |
| 0.01 | 5.11 | 0.196 | 33.33 |
| 0.001 | 0.511 | 1.96 | 333 |

## 6.3   Band Specific PRBS Design

To further illustrate how PRBS parameters can be strategically selected to target specific frequency regions, two configurations were evaluated:

- Low frequency emphasis: 12-bit, $T_c = 0.1$ s
- High frequency emphasis: 6-bit, $T_c = 0.001$ s
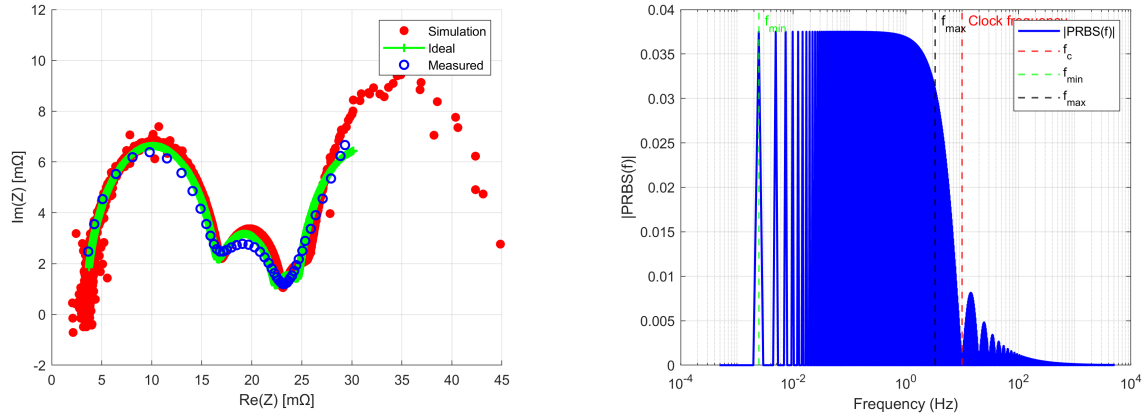
***Figure 6.6.*** Nyquist and FFT plot of the 12-bit generator with $T_c = 0.1$ s.

The 12-bit, slow clock PRBS produces a long sequence with a duration of over 400 seconds and a minimum frequency down to 2.44 mHz. This configuration provides excellent coverage of the diffusion region and enables estimation of very slow electrochemical dynamics. However, the long simulation time and relatively low maximum frequency (3.33 Hz) introduces noise into the ohmic and charge transfer process.
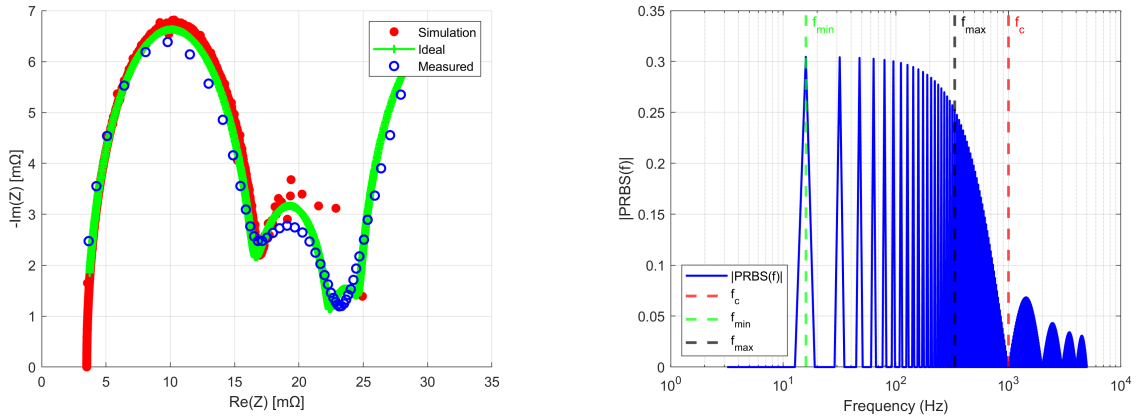


***Figure 6.7.*** Nyquist and FFT plot of the 6-bit generator with $T_c = 0.001$ s.

The 6-bit fast clock configuration is the opposite, with a duration of only 63 ms, it covers up to 333 Hz but only reaches down to 16 Hz. As such, it captures the high frequency region of the impedance spectrum effectively, particularly the ohmic resistance, but is unable to provide meaningful insight into the mid or low frequency dynamics.

***Table 6.3.*** PRBS parameters for different configurations of bit length and clock period.

| Bit Length $n$ | Clock Period $T_c$ (s) | PRBS Duration (s) | $f_{\min}$ (Hz) | $f_{\max}$ (Hz) |
|:---:|:---:|:---:|:---:|:---:|
| 12 | 0.1 | 409.5 | 0.00244 | 3.33 |
| 9 | 0.01 | 5.11 | 0.196 | 33.33 |
| 6 | 0.001 | 0.063 | 15.87 | 333.33 |

# Discussion 7

## 7.1 PRBS Design Tradeoffs

As demonstrated in Section 6.1, the bit length of the PRBS signal plays a crucial role in determining the low frequency resolution of the impedance spectrum. A longer bit length results in a lower minimum frequency but also leads to significantly longer PRBS durations. For instance, a 12-bit PRBS corresponds to a sequence duration of approximately 205 seconds per period. To improve spectral averaging, five periods were simulated, extending the total duration to around 1020 seconds. This increase has a substantial impact on simulation time, especially when combined with a smaller clock period, $T_c = 0.1\,\mathrm{s}$, which doubled the overall duration and nearly exhausted system memory.

These tradeoffs highlight the importance of aligning PRBS configurations with the specific objectives of the impedance analysis. For example, while a longer bit length enables better resolution of the low frequency (diffusion) region of the impedance spectrum, it comes at the cost of significantly higher measurement time. Since one of the primary advantages of PRBS based impedance estimation is the potential for short measurement times, it is essential to evaluate whether capturing the full diffusion arc is necessary for a given application. Additionally, at higher bit lengths, the results exhibited increased noise, potentially degrading the accuracy of the impedance estimation.

To extend the bandwidth and capture higher frequency behavior, the clock period $T_c$ must be reduced. A shorter $T_c$ increases the maximum frequency of the PRBS excitation and shortens the overall sequence duration, helping to offset the longer sequences from high bit lengths. However, this comes with computational costs: a smaller $T_c$ results in a higher sampling rate, generating larger data files and placing greater demands on memory and processing resources, particularly during FFT based analysis. In some simulations, specifically the 12-bit sequence with $T_c = 0.1\,\mathrm{s}$ in Section 6.3, memory issues were encountered. While this can be mitigated through memory optimization techniques, it remains an important consideratios for real time or embedded implementations.

Amplitude scaling of the PRBS signal is another design parameter of practical importance, particularly in real world systems where safety and signal to noise ratio must be balanced. In simulation, varying the PRBS amplitude did not lead to substantial improvements in impedance estimation quality, likely due to the absence of measurement noise. However, in experimental context, where noise is present, a carefully chosen amplitude becomes critical to ensuring sufficient excitation without compromising system stability or component safety.

## 7.2  Impedance Estimation Accuracy

The accuracy of the impedance estimation in simulation is fundamentally limited by how well the battery model represents the actual system. As show in Figure 5.2 in Section 5.1, the theoretical impedance, calculated from the transfer function of the battery model, matches the measured impedance from EIS reasonably well, particularly in the high and mid frequency regions. However some discrepancies appear in the second semi circle and the early part of the diffusion region. These deviations likely stem from the model limitations. A more complex ECM could potentially improve this match, but the focus of this project is not on refining battery modelling accuracy, but rather on evaluating the effectiveness of PRBS based impedance estimation.

Because the simulations are based purely on the implemented model, the resulting impedance estimates are compared against the theoretical model response rather than the experimental EIS measurements. In a real world validation scenario, the estimated impedance would instead be benchmarked against actual measured data to evaluate accuracy.

The simulation results show that the PRBS based approach captures the impedance well across the high and mid frequency regions of the Nyquist plot. However, extracting reliable impedance data from the low frequency region requires either a high PRBS bit length or a small clock period $T_c$. This suggest that achieving a sufficiently low $f_{min}$ is crucial for resolving the diffusion tail in the impedance spectrum. On the other hand, increasing the frequency content introduced some high frequency noise, but its impact appeared less severe than the limitations observed at the low frequency end.

Interestingly, the simulation also provided impedance estimation in the high frequency region beyond the range of the available EIS measurements data. While EIS systems are in principle capable of capturing this region, it was not included in the specific measurement used for comparison. This highlights how simulation, when based on a well defined battery model, can offer a more continuous and extended impedance spectrum, useful for exploring system behaviour outside the measured bandwidth.

## 7.3  Simulation vs. Reality

As no experimental validation was carried out, the PRBS signal design and impedance estimation in this study are based entirely on theoretical analysis and simulation. While the simulation results demonstrate the feasibility of using PRBS for impedance estimation, the real world application remains uncertain. Factors such as measurement noise, inverter dynamics and limited sampling accuracy could significantly impact performance in a physical system.

In particular, the signal to noise ratio is expected to pose a much greater challenge in practice. In simulation, the absence of noise allowed for clean excitation and response signals, but in reality, electrical noise and disturbances may obscure the battery voltage response, especially at high frequencies or low PRBS amplitudes. As such, parameters like amplitude scaling, while having minimal effect in simulation, would become critical design considerations in an actual implementation. Amplitude must be selected carefully to provide sufficient excitation for accurate impedance estimation, while remaining within safe operational limits for both the battery and motor controller.

Overall, the lack of experimental testing means that some conclusions, particularly those related to low frequency estimation quality or PRBS amplitude effects, should be interpreted cautiously. Future work should aim to validate the method on real hardware, where the interplay of noise, system delays and nonlinearities can be properly accounted for.

# Conclusion 8

This project explored the use of Pseudo Random Binary Sequence (PRBS) signals for online battery impedance estimation in motor driven systems. The motivation stems from the limitations of traditional Electrochemical Impedance Spectroscopy (EIS) in real time applications, particularly within electrical vehicles. By injecting PRBS signals into the motor control loop and analysing the resulting battery voltage and current, the feasibility of real time impedance estimation was investigated through simulation.

A 4-RC battery model was used to simulate the impedance behaviour, and various PRBS configurations were evaluated to understand their impact on estimation quality. The study showed that key parameters, bit length, clock frequency and amplitude, directly affect the frequency range and accuracy of the estimated impedance.

Longer bit lengths improved resolution in the low frequency diffusion region but increased simulation time and noise. Conversely, higher clock frequencies allowed better capture of the ohmic and charge transfer region but limited access to lower frequencies. While amplitude scaling had little impact in simulation due to the absence of noise, it is expected to be critical in practical applications.

Overall, the simulations confirmed the PRBS signals can successfully be used for impedance estimation across a wide frequency range, provided the PRBS design is carefully tailored. The results also emphasized the trade-offs between estimation accuracy, frequency coverage and measurement duration. Although no experimental work was conducted, the simulation results provide a solid foundation for future implementation and testing on real systems.

## 8.1 Further work

Due to time constraints, it was not possible to carry out real world testing, which is one of the primary limitations of this work. Therefore the most important next step would be to implement and test the PRBS injection method on an actual system. Factors such as measurement noise and inverter switching behaviour are expected to have a significant impact, for experimental work. These effects are not captured in simulation and could strongly influence the accuracy and reliability of the impedance estimation.

As an intermediate step before implementing the PRBS signal into an experimental setup with a battery motor system, it would be valuable to test the signal on a battery cell beforehand. This can be done on Neware hardware that would allow a predefined current signal to be applied to the battery cell and would log voltage and current signal. Insights from this test could guide necessary adjustment to the PRBS design before attempting implementation in a motor driven setup.

# Bibliography

[1]  International Energy Agency. *Global EV Outlook 2023: Trends in Batteries*. Last checked: 28-04-2025. 2023. URL: `https://www.iea.org/reports/global-ev-outlook-2023/trends-in-batteries`.

[2]  Sergio Vazquez. *Energy Storage Systems for Transport and Grid Applicationss*. Last checked: 12-05-2025. 2010. URL: `https://citeseerx.ist.psu.edu/document?repid=rep1&type=pdf&doi=fefdae36f5d4e8de5fe80ee2fc03dc42d9d014d5`.

[3]  Jussi Sihvo et al. *A Fast Approach for Battery Impedance Identification Using Pseudo Random Sequence (PRS) Signals*. `https://vbn.aau.dk/ws/portalfiles/portal/308357662/A_Fast_Approach_for_Battery_Impedance_Identification_Using_Pseudo_Random_Sequence_PRS_Signals.pdf`. Last checked: 25-02-2025. 2020.

[4]  Instruments Gamry. *Basics of Electrochemical Impedance Spectroscopy*. `https://www.gamry.com/application-notes/EIS/basics-of-electrochemical-impedance-spectroscopy/`. Last checked: 28-05-2025.

[5]  Marzia Abaspour, Krishna R. Pattipati and Behnam Shahrrava. *Robust Approach to Battery Equivalent-Circuit-Model Parameter Extraction Using Electrochemical Impedance Spectroscopy*. `https://www.mdpi.com/1996-1073/15/23/9251`. Last checked: 16-05-2025. 2022.

[6]  A.J. Fairweather, M.P. Foster and D.A. Stone. *Battery parameter identification with Pseudo Random Binary Sequence excitation (PRBS)*. `https://www.sciencedirect.com/science/article/pii/S0378775311013097`. Last checked: 12-05-2025. 2011.

[7]  Daniel Alby et al. *Battery Impedance Estimation Using Kalman Filters, Recursive Least Squares Method and Field-Oriented Control with a PMSM*. Tech. rep. AAU, 2024.